J. Synchrotron Rad. (1995). **2**, 49–55

Rapid Mapping of Texture in Polycrystalline Materials Using an Imaging Plate on a Synchrotron Radiation Source

K. Kawasaki[a] and H. Iwasaki[b]*

[a]*Advanced Materials and Technology Research Laboratories, Nippon Steel Corporation, 1618 Ida, Nakahara-ku, Kawasaki, Kanagawa 211, Japan, and* [b]*Photon Factory, National Laboratory for High Energy Physics, Tsukuba, Ibaraki 305, Japan*

(*Received 15 July 1994; accepted 6 October 1994*)

Taking advantage of the high brilliance of synchrotron radiation, a system was developed for rapid mapping of the orientation distribution of crystal grains (texture) in polycrystalline materials using an imaging plate. A monochromatized beam is incident on the sample, which is rotated using the ω-axis mechanism of an X-ray diffractometer so that the surface of the sphere of poles of the selected reflection is scanned by the Ewald sphere. Simultaneously, the imaging plate is translated vertically with a velocity that is synchronized with that of the sample rotation. It is possible to record pole figures over an extended angular range within a short period of time, typically of the order of minutes. The method has been applied to the observation of a time change in the orientation distribution of metal sheets at elevated temperatures.

Keywords: texture; X-ray diffraction; dynamic observation; polycrystalline materials.

1. Introduction

Metals and alloys are important materials in modern industries. They are in most cases in a polycrystalline state, and rolled to form sheets (plates) or extruded to form wires (bars). It is well known that magnetic, mechanical or corrosion properties of the materials depend on the orientation distribution of crystal grains, called texture, which is formed during the process of rolling or extrusion and subsequent heating. It is important to have information on the texture for the successful use of metals as engineering and functional materials.

There is a traditional convention for representing the texture, known as a pole figure (Barrett, 1952). It is usually determined by means of X-ray diffraction analysis: the sample material is fixed on the goniometer and a diffraction peak from a particular set of planes is measured using a detector, while simultaneously changing the orientation of the sample. Plotting the polar and azimuthal angles at which the diffraction peak is detected onto the surface of the sphere of poles yields the orientation distribution of the set of planes for all crystal grains in the sample irradiated by the X-rays. This is a kind of 'point-by-point method' and is, in general, time-consuming. In addition, the resolution of the measured distribution is not high unless the angular steps of sample rotation are small.

Investigations (Guinier & Tennevin, 1948; Milner & James, 1953) were made to record the pole figure without recourse to the point-by-point method. A special camera was designed, using an X-ray film as a two-dimensional detector. However, owing to the lack of a powerful X-ray source at that stage, the time required for the recording was excessively long and the method has not, therefore, been used extensively.

Recent development of synchrotron radiation sources provides an intense X-radiation for materials research. In addition, the invention of a highly sensitive X-ray 'film' imaging plate (Miyahara, Takahashi, Amemiya, Kamiya & Satow, 1986) gives the possibility of considerably shortening the recording time. We have developed a method of rapid mapping of texture in metallic sheets by combining the use of synchrotron radiation and the imaging plate. It is, in a sense, a revival of the method developed previously, but enables us not only to map texture but also to observe its change with time.

The outline of the method and some results of mapping are described below.

2. Method

The pole figure is represented as a distribution of the diffraction intensity from a particular set of planes onto the surface of the sphere of poles. Fig. 1 shows this sphere in relation to the Ewald sphere. The mapping is made by rotating the sphere of poles around a certain axis so that the intersection with the Ewald sphere continuously sweeps the surface of the sphere of poles. Since there are concentric spheres of poles with different radii corresponding to other kinds of atomic planes, and their surfaces are also intersected by the Ewald sphere, a screen should be placed to select the diffracted radiation from the atomic plane under

* Present address: Department of Physics, Faculty of Science and Engineering, Ritsumeikan University, Kusatsu, Shiga 525, Japan.

investigation. Behind the screen, the two-dimensional detector is fixed on a moving stage which undergoes a vertical translation motion with the velocity synchronized with the sample rotation velocity.

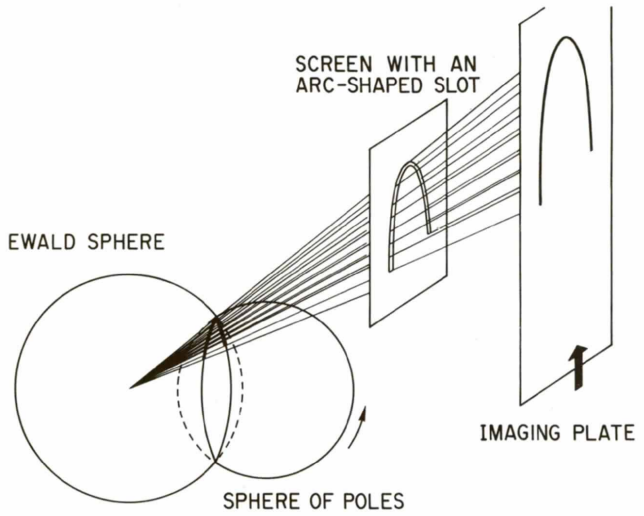

Figure 1
Diagram showing the principle of X-ray diffraction mapping of texture in polycrystalline materials. The sample (and the associated sphere of poles) is rotated and a two-dimensional detector is translated vertically. A screen is placed between the sample and the detector to select the radiation diffracted from a particular set of planes.

The radiation emitted from the bending magnet in the 2.5 GeV storage ring at the Photon Factory, National Laboratory for High Energy Physics, was used for the diffraction measurements and was monochromatized by reflection from a pair of silicon (111) crystals and collimated to form a beam 4×4 mm in cross section. The angular divergence of the beam was 10 mrad in the horizontal plane. The photon flux at the sample position was 1.3×10^{10} photons $s^{-1}\,mm^{-2}$ at the wavelength of 0.06 nm, when the storage ring was operated with a beam current of 250 mA. A four-circle X-ray diffractometer (Kawasaki, Takagi, Nose, Morikawa, Yamazaki, Kikuchi & Sasaki, 1992) installed at the BL-3A beamline was employed. The sample, in the form of a sheet 70 mm in length, 10 mm in width and 0.1–1.0 mm in thickness, was fixed on the sample stage of the diffractometer and rotated using the the ω-axis rotation mechanism. The screen, made of steel plate, was placed between the sample and the detector, whose position could be adjusted so that selected diffracted radiation could pass through. The size of the scanned area on the surface of the sphere of poles was determined by the angle range of the sample rotation and the length of the arc-shaped slot in the screen. Transmission geometry was adopted in the present diffraction measurement and the maximum angular range of the sample rotation was 60° in longitude and the screen had a quarter-circle slot. If the sample materials are based on the face-centred cubic or body-centred cubic metals, the pole figure has a higher symmetry, and scanning over a part of the surface of the

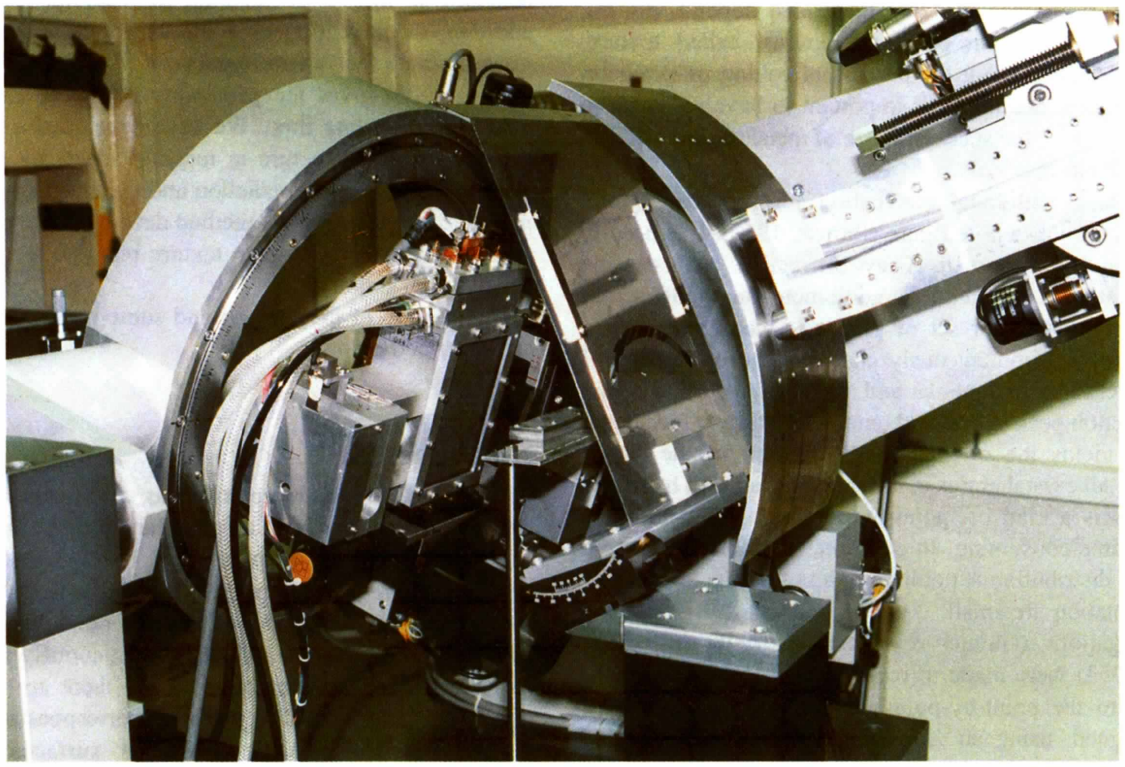

Figure 2
A photograph of the system used for texture mapping developed in this study and installed at the BL-3A beamline at the Photon Factory.

sphere of poles is sufficient to construct a pole figure. The imaging plate, 400 mm in length and 200 mm in width, was enclosed in the bent plate cassette, which was fixed on the 2θ arm of the diffractometer. The translation motion (frame shifting) of the imaging plate was performed using the rotation mechanism of the 2θ axis. The pattern recorded on the imaging plate was reproduced either on the display screen of the imaging plate reader or on photo-sensitive chart paper. Since the pattern is a projection of the intensity distribution on the spherical surface onto a flat plane, a distortion is inevitably introduced into the projected pole figure. For the reconstruction of undistorted pole figures, the mathematical relation between the coordinates on the spherical surface and those on the projection plane derived previously (Guinier & Tennevin, 1948) may be used.

Fig. 2 shows a photograph of the actual system used for the texture mapping developed in the present study.

3. Results

3.1. *Mapping of the texture of cold-rolled and annealed metal sheets*

Fig. 3(*a*) shows a pattern using the 111 diffraction peak from a cold-rolled aluminium alloy sheet with the face-centred cubic structure. The wavelength of monochromatized radiation was 0.06 nm ($2\theta = 14.74°$) and the angular range of the sample rotation was 40°. The sample thickness was 1 mm and it took 80 s to collect a pattern. For the sake of comparison the (111) pole figure obtained for a similar cold-rolled sheet by a conventional point-by-point method is shown in Fig. 4. The area scanned by the present mapping method is indicated by broken lines. The two peaks located around the north pole in Fig. 4 (the polar axis being chosen parallel to the rolling direction) are characteristic of the [111] pole figure of cold-rolled aluminium alloy sheets, and they appear as two black broad maxima at the top of Fig. 3(*a*). Immediately below the two peaks in Fig. 4, there is a region with lower density of the [111] poles, which appears as a large white circular area in Fig. 3(*a*).

When the sheet was annealed at 800 K for 1 min, the pattern changed appreciably, as shown in Fig. 3(*b*). The broad maxima around the north pole disappeared and a rather uniform distribution of the [111] poles formed, with a slightly higher density in the region where the density was low in the as-cold-rolled state. It is notable in Fig. 3(*b*) that the pattern consists of numerous tiny spots in place of the continuous black–white contrast in Fig. 3(*a*). This shows that recrystallization took place during the annealing, and the lattice distortion introduced by the cold rolling was removed. The advantage of the mapping method over the point-by-point method is that it reveals not only the change in the orientation distribution of crystal grains, but also the change in the lattice distortion.

Another example of the mapping is shown in Fig. 5 for a silicon steel sheet. The pattern was obtained using the 200 diffraction peak of the body-centred cubic structure ($2\theta = 24.17°$). The sample thickness was 0.2 mm and the angle range of the sample rotation was 40° in longitude. The sheet had been annealed after cold rolling with the result

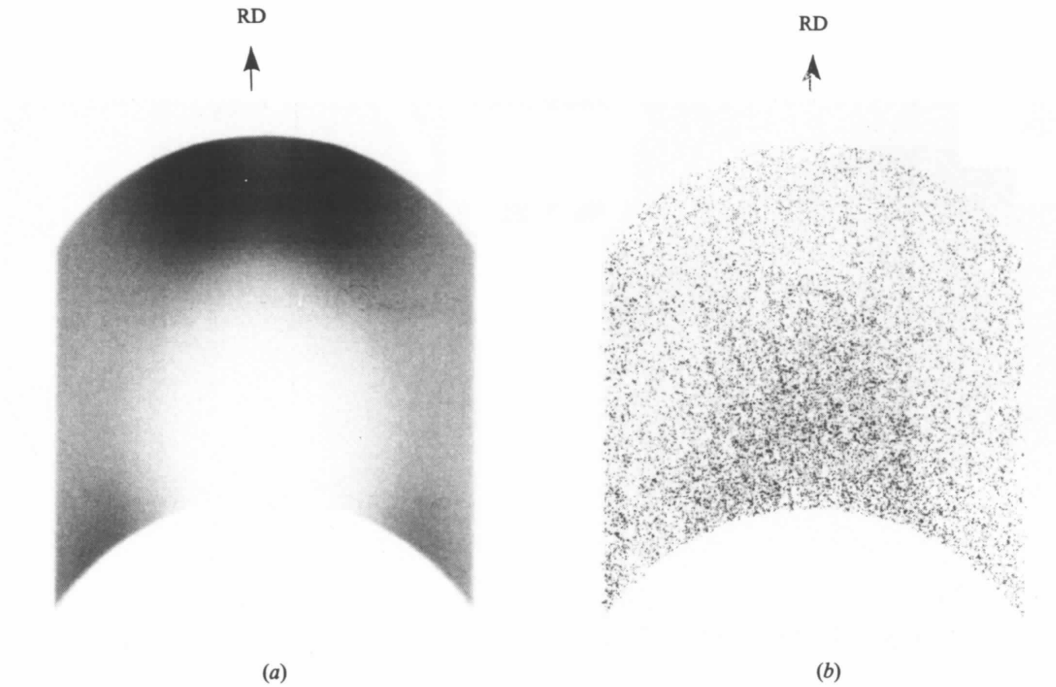

Figure 3
Mapping patterns of the [111] poles of an aluminium alloy sheet, (*a*) in the cold-rolled state and (*b*) in the annealed state. The angular range of the sample rotation was 40° in longitude. The wavelength of the radiation used was 0.06 nm ($2\theta = 14.74°$). The time required to record each pattern was 80 s. RD represents the rolling direction.

that recrystallization occurred (primary recrystallization). A broad maximum is seen at the top, *i.e.* at the north pole (rolling direction).

3.2. *Observation of the changes in the orientation distribution of crystal grains at high temperatures*

The short period of time required for recording a pattern enables us to apply the method of mapping to dynamic observations of the changes in texture. For this purpose, the area on the surface of the sphere of poles to be observed must be defined. Fig. 6(*a*) shows the [200] pole figure of the silicon steel after primary recrystallization and a region around the north pole (shown shaded) was chosen, since an appreciable change was expected in that region when the sheet was heated. In order to follow rapid changes, the angular range of the sample rotation was set to be small, 10°, and the scanning rotation was repeated while the sample was maintained at elevated temperatures. On the other hand, the imaging plate was set to follow a continuous translation motion.

The high-temperature sample stage employed was designed by Kawasaki (1992). It has a large X-ray window made of beryllium and carbon sheet with a device to apply tensile stress to the sample during annealing.

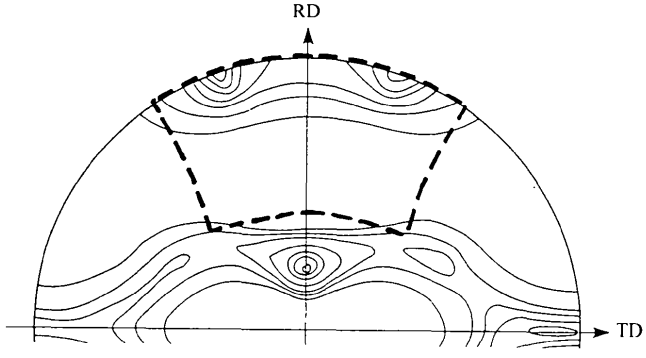

Figure 4
The [111] pole figure of a cold-rolled aluminium alloy sheet obtained by a conventional point-by-point method. The area scanned by the method of mapping is indicated by broken lines. RD represents the rolling direction and TD the traverse direction.

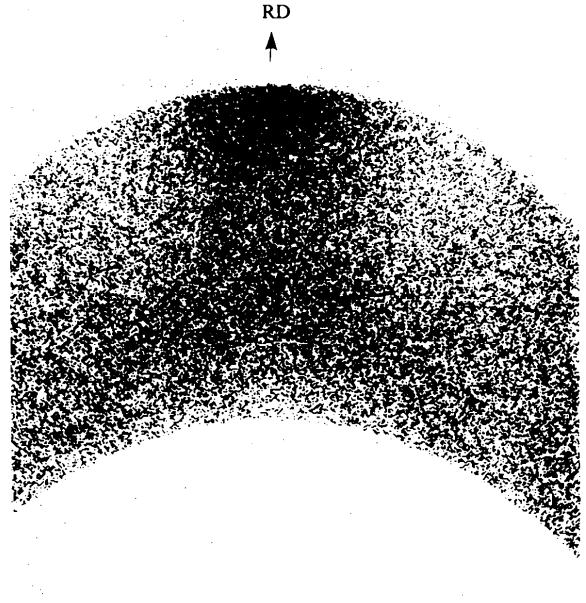

Figure 5
A mapping pattern of the [200] poles of a silicon steel sheet, which was in a recrystallized state (primary recrystallization). The measurement condition was the same as that in Fig. 3 ($2\theta = 24.17°$).

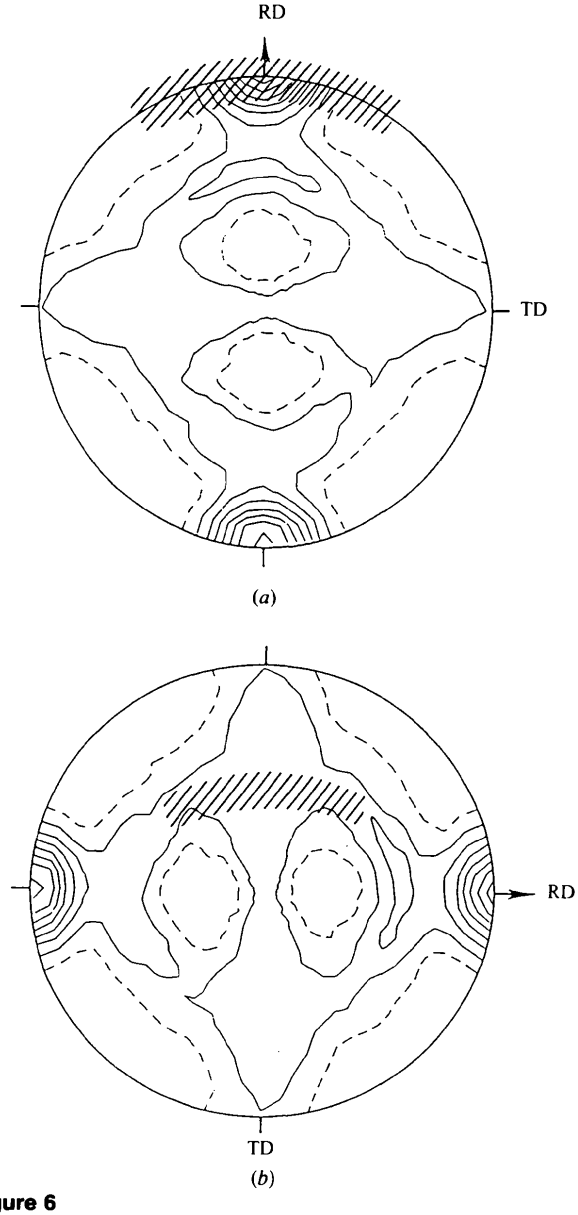

Figure 6
The [200] pole figures of a recrystallized silicon steel sheet, (*a*) showing the region around the north pole scanned first (shaded) and (*b*) showing the region across the equator scanned afterwards.

Fig. 7 is a series of the patterns thus obtained, showing the time change in the distribution of the [200] poles around the north pole of the silicon steel sheet, kept at a temperature of 1233 K. The wavelength of radiation used was 0.06 nm. It took 40 s to obtain each arc-shaped pattern and 80 s to set the sample back to the initial position and start the next recording. The pattern at the bottom in Fig. 7 is that obtained immediately after the sample temperature reached 1233 K. Comparison with the pattern shown in Fig. 5 shows that no appreciable change occurred in the orientation distribution of crystal grains during the initial stage of the annealing. The second arc-shaped pattern in Fig. 7 is that obtained after 120 s annealing at 1233 K, after which the pattern still remained unchanged. However, a sudden change in the orientation distribution began after 240 s annealing, resulting in the formation of a sharp maximum at the north pole, as seen in the third pattern. This suggests that grain growth took place with a preferred orientation of the [200] poles in the rolling direction. This change is known as secondary recrystallization of the silicon steel sheet. The height of the maximum gradually increased with a further elapse of annealing time. Tiny spots distributed sparsely in the other region of the pattern represent the remaining smaller crystal grains with almost random orientation.

Next, another dynamic observation was made for the region located across the equator in the [200] pole figure, as shown in Fig. 6(*b*). For this observation, the sample was cut from the original sheet with an orientation perpendicular to that of the sample used in the first observation. In Fig. 8, a series of patterns shows the time change in the second region in the pole figure at 1233 K. In this region, no maximum or minimum was present in the initial state. It can be seen that an incubation period existed at the beginning whilst no change was observed in the grain orientation distribution. After 240 s an explosive concentration of the grain orientation occurred, with a maximum appearing in the central region of the arc-shaped pattern.* The maximum gradually increased on further annealing. Judging from the

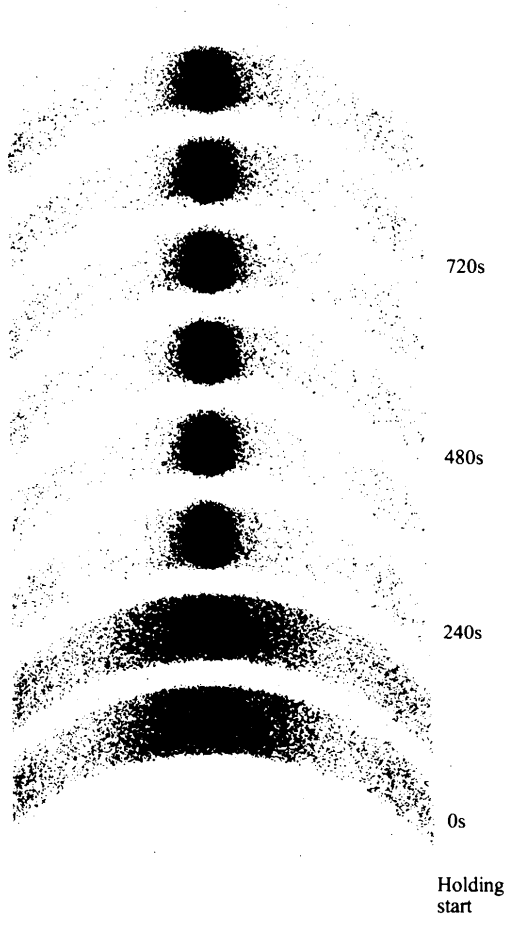

Figure 7
A series of mapping patterns showing the time change in the orientation distribution of the [200] poles of a silicon steel sheet during secondary recrystallization at 1233 K. Each arc shows the distribution over an angle range of 10° in longitude around the north pole. The pattern at the bottom is that obtained immediately after the sample temperature reached 1233 K. Figures on the right-hand side represent the time the sample was held at 1233 K. There is an incubation period for the onset of secondary recrystallization. The wavelength of radiation was 0.06 nm. The exposure time for each pattern was 40 s.

*Note that the incident angle of radiation to the sample was different from that in Fig. 7 and therefore the effect of absorption was different.

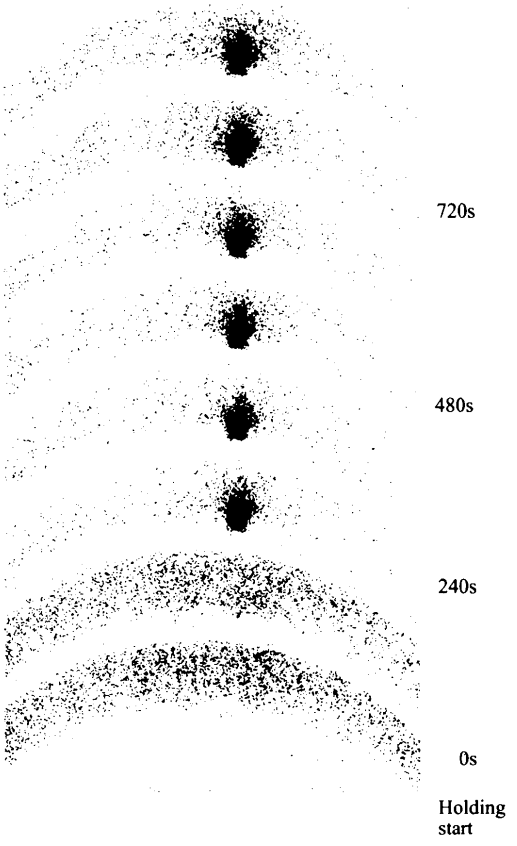

Figure 8
A series of mapping patterns showing the time change in the orientation distribution of the [200] poles of a silicon steel sheet during secondary recrystallization at 1233 K. Each arc shows the distribution over an angle range of 10° in longitude across the equator. The others are the same as those in Fig. 7.

location of the two kinds of maxima in the patterns, the secondary recrystallization in the silicon steel sheet is seen to give rise to large crystal grains with an orientation such that the (011) planes of the body-centred cubic lattice structure are parallel to the sheet surface and the [100] direction is in the rolling direction. This orientation is simply the Goss orientation which is known to be favorable for the reduction of iron loss in silicon steel sheet (Goss, 1934).

The third dynamic observation was to observe the effect of a tensile stress on secondary recrystallization. A similar sample to that used in the observation shown in Fig. 8 was used. Application of the tensile stress started while the sample temperature was increasing, and the sample was loaded in the traverse direction (TD) in Fig. 6(*b*) at a strain rate of 1 μm s^{-1}. The sample was held under stress during the 1233 K annealing. The highest magnitude of strain was 2%. Fig. 9 shows a series of patterns obtained under this tensile stress. The effect was so strong that changes in grain orientation were completely suppressed, as seen in the first four arc-shaped patterns in Fig. 9. When the stress was released, at 300 s, the maximum gradually appeared and grew.

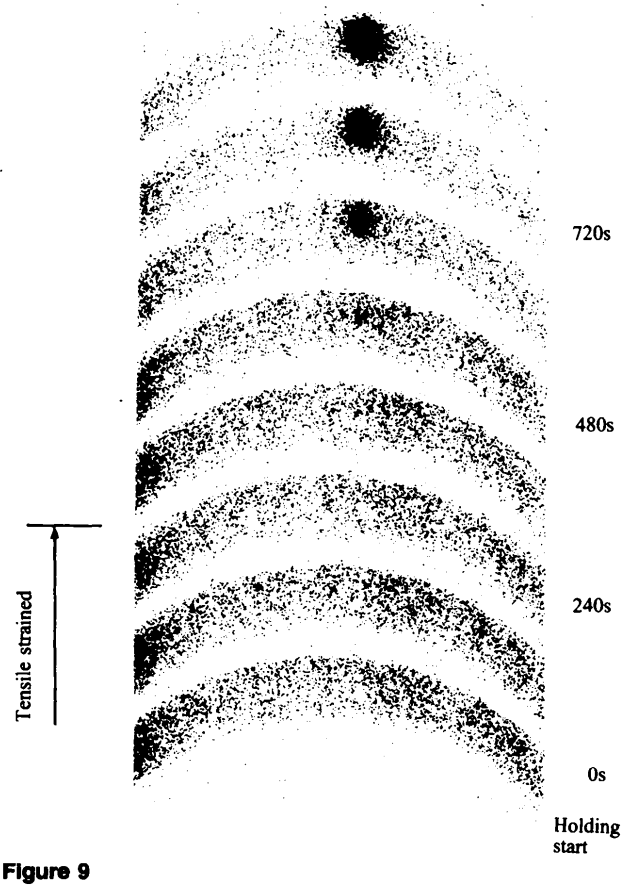

Figure 9
As Fig. 8, except that a tensile stress was applied to the sample from the start of holding at 1233 K and released at 300 s. It can be seen that there is an appreciable delay in the onset of secondary recrystallization.

3.3 *Close-up inspection of the patterns in the incubation period*

The results of the observations described above reveal that at the initial stage of annealing a period exists in which no change occurs in the grain orientation. Attempts were made to inspect the distribution of the spots during this period in more detail within a magnified image. Fig. 10 shows the images obtained with the magnification mechanism of the imaging plate reader (using a magnification of 8). They have been taken from the small area in the centre of the first four arc-shaped patterns in Fig. 9. The spots are the 200 diffraction peaks from the crystal grains of the silicon steel sheet before secondary recrystallization. Close inspection has shown that there are the same number of spots in the four magnified images but that the intensity and size of some of the spots do not necessarily remain the same. The arrows on the images indicate the spots which show variations in intensity and size. This fact suggests that there is a fluctuation in the degree of perfection and size of crystal grains before the onset of appreciable grain growth: it is reminiscent of the fluctuations which occur in solids prior to a structural phase transition.

4. Discussion

The time required for taking a pattern of texture mapping is determined primarily by the intensity of the incident radiation and the sensitivity of the detector. Use of the radiation emitted from a multipole wiggler will considerably shorten the time, and the method may be applicable to the dynamic observation of even more rapid changes in texture. For the detector, the imaging plate used in the present work is of the integration type. Recently, a detector of the pulse-counting type with sensitivity and spatial resolution

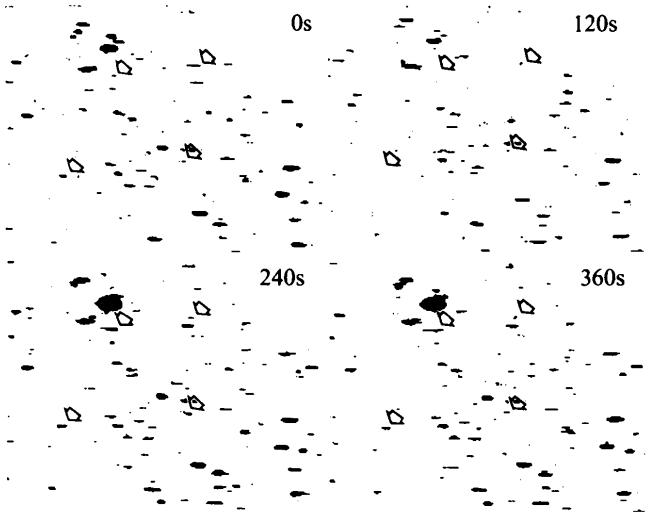

Figure 10
Magnified images of the central region of the first four patterns in Fig. 9, showing fluctuation in the intensity and size of diffraction spots (indicated by the arrows) during the incubation period.

comparable with the imaging plate has been developed (Moy, 1993), which will be more suitable for real-time measurements.

The transmission geometry was adopted in the present method of texture mapping. It is not possible to scan the whole surface area of the sphere of poles with this geometry, and a reflection geometry may be adopted to investigate the distribution of poles in the central area of the circle of the pole figure. The system described in this paper allows one to adopt both types of geometry. However, care must be taken with regard to the difference between the sample volumes irradiated by the incident radiation in the two types of geometry.

The present method can be applied to the observation of any changes in the orientation and size of crystal grains in materials, not only at elevated temperatures and under tensile stress, but also in electric or magnetic fields. Metallic wires, ceramic sheets and sintered plates may also be used as samples.

The present work was performed under the approval of the Photon Factory Program Advisory Committee (proposal No. 91-265). The authors wish to thank Dr Y. Sakuma and Mr T. Shimazu of Nippon Steel Corporation for providing the samples used in this study.

References

Barrett, C. S. (1952). *Structure of Metals,* 2nd ed., pp. 170–195. New York: McGraw-Hill.

Goss, N. P. (1934). US Patent 1 965 559.

Guinier, A. & Tennevin, J. (1948). *Rev. Met.* **45**, 277–286.

Kawasaki, K. (1992). PhD Thesis, Graduate Univ. for Advanced Studies, Japan.

Kawasaki, K., Takagi, Y., Nose, K., Morikawa, H., Yamazaki, S., Kikuchi, T. & Sasaki, S. (1992). *Rev. Sci. Instrum.* **63**, 1023–1026.

Milner, C. J. & James, J. A. (1953). *J. Sci. Instrum.* **30**, 77–38.

Miyahara, J., Takahashi, K., Amemiya, Y., Kamiya, N. & Satow, Y. (1986). *Nucl. Instrum. Methods,* A**246**, 572–578.

Moy, J. P. (1993). *ESRF Newsl.* (18), 8–9.